ChemComm

COMMUNICATION

View Article Online
View Journal | View Issue

Cite this: *Chem. Commun.*, 2019, 55, 3469

Received 5th February 2019,
Accepted 25th February 2019

DOI: 10.1039/c9cc01068h

rsc.li/chemcomm

Red-emitting pyrene–benzothiazolium: unexpected selectivity to lysosomes for real-time cell imaging without alkalinizing effect†

Chathura S. Abeywickrama,[a] Kaveesha J. Wijesinghe,[b] Robert V. Stahelin [c] and Yi Pang *[ad]

A series of pyrene–benzothiazolium probes were synthesized. By replacing the pyridinium with a benzothiazolium unit, the selectivity of pyrene-derivatives is found to switch from nuclear to cellular lysosomes. New probes do not require proton participation and exhibit high biocompatibility and long-term imaging ability.

Lysosomes are membrane-encapsulated organelles that contain degradative enzymes to digest macromolecules within the cell.[1,2] Since the discovery of lysosomes by Duve in 1955,[3] the organelles are known to contain a variety of digestive enzymes called "hydrolases", which exhibit optimal activity in a narrow acidic pH environment within the lysosomal lumen (pH 4.5–6).[4] Abnormal lysosome activities or lysosome malfunction has been attributed to many disease conditions including neurodegenerative disorders, lysosome storage diseases, cancer and inflammations.[4–13]

Imaging lysosomes in live or fixed cell samples has recently received much attention due to their involvement in cell processing activities and cancer.[12,14–17] Most probe design incorporates a basic amino group for lysosome selectivity, which include commercial LysoTracker® Green DND-26 (λ_{ex} ~ 504 nm, λ_{em} ~ 510 nm) and LysoTracker® Red DND-99 (λ_{ex} ~ 577 nm, λ_{em} ~ 590 nm).[18] Since the existing fluorescent probes require an acidic media to operate, their accumulation in lysosomes will cause the pH increase (the "alkalinizing effect") that perturbs the normal cell activity.[19–22] Although new lysosome probes have been developed recently with spirolactams[23] and peptide[24] based molecules, protonation of an amine group remains an essential step, in order to guide the probe molecules into the acidic lysosome lumen. There are also interests in developing new probes that exhibit emission in the near infrared (NIR) region.[24–26] However, no lysosome probes are found to operate without resorting to protonation in the lumen, which is known to alter the intracellular pH to affect normal cell activities.

As a planar molecular skeleton with extensive conjugation, pyrene has been used for developing fluorescent sensors,[27–32] including those for intracellular membranes[30] and mitochondria.[31] Our recent study shows that probe **1** is a bright red-emitting dye for cell nucleus staining.[32] The nucleus selectivity of **1** is likely achieved *via* binding to DNA minor grove (Fig. 1a). During the interaction, the ammonium cation is assumed to fit into the shallow space of the DNA minor grove for effective polar interaction with the DNA backbone. In an effort to examine the substituent impact on the cell staining, herein we report the synthesis of **2**, where the substituent R on the benzothiazolium could provide sufficient steric hindrance to prevent the ammonium cation to fully enter the DNA minor grove, thereby decreasing its interaction with the cell nucleus. Surprisingly, compound **2** exhibited remarkable

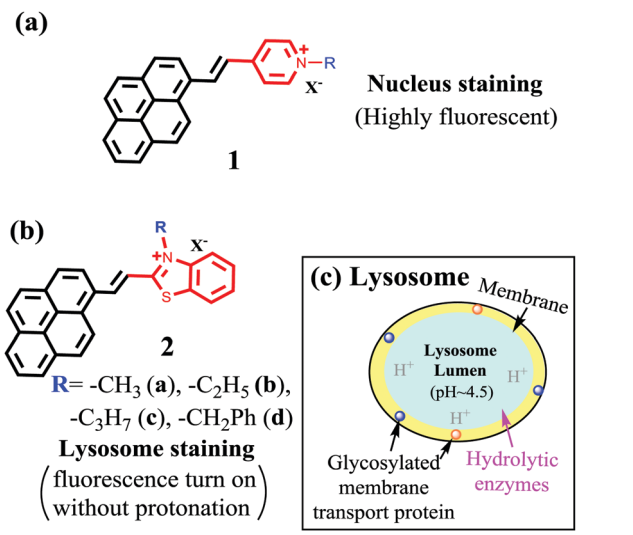

Fig. 1 Structure of pyrene-based probes **1** (a) and (b) **2** and their selectivity switch from nucleus to lysosomes. And schematic illustration of lysosome structure (c).

[a] *Department of Chemistry, University of Akron, Akron, Ohio 44325, USA. E-mail: yp5@uakron.edu*
[b] *Department of Chemistry and Biochemistry, University of Notre Dame, Notre Dame, Indiana, USA*
[c] *Department of Medicinal Chemistry and Molecular Pharmacology, Purdue University, West Lafayette, Indiana, 47907, USA*
[d] *Maurice Morton Institute of Polymer Science, University of Akron, Akron, Ohio 44325, USA*

† Electronic supplementary information (ESI) available. See DOI: 10.1039/c9cc01068h

selectivity for intracellular lysosomes, in sharp contrast to **1**. Since **2** has no group for protonation, its ability to generate bright red fluorescence, upon binding to lysosomes, provides a promising strategy to achieve long term tracking of lysosomes by eliminating harmful ''alkalinizing effects''.

Synthesis: The probe **2** with different substituents was synthesized in good yields (ESI,† Fig. S1).[26,32] Chemical structures of probe **2** were characterized by ^{1}H NMR and ^{13}C NMR spectroscopy and high-resolution mass spectrometry (ESI,† Fig. S2 and S3).

Optical properties: In dichloromethane (DCM), probes **2** exhibited $\lambda_{abs} \approx 530$–$540$ nm (Table 1 and ESI,† Fig. S4), which, is significantly red-shifted from the monomeric pyrene ($\lambda_{abs} \approx 352$ nm). The observed large bathochromic shift could be attributed to the strong intra-molecular charge transfer (ICT) from pyrene to benzothiazolium moiety in **2**, which was verified by spectroscopic study at low temperature (in liquid nitrogen at −188 °C) (ESI,† Fig. S5). The probe **2** also showed bright red emission with $\lambda_{em} \sim 630$–640 nm ($\phi_{fl} \approx 0.22$–0.48 in DMSO), along with a large Stokes' shift ($\Delta\lambda \approx 140$ nm, 4170 cm^{-1}). Interestingly, fluorescent quantum yield of **2** was significantly lower in an aqueous environment ($\phi_{fl} \approx 0.05$) than that in a non-aqueous media (Table 1), making it possible for cell staining under ''wash-free'' conditions.

Biological cell studies: Bright red emission was observed when using **2** (500 nM) to stain different cell lines (COS-7, HEK293, A549 and Huh 7.5) (ESI,† Fig. S7). Clear cell imaging was observable after 30 minutes of staining without any post-staining washing. The non-uniform pattern observed from the cell imaging (Fig. 2) suggested that the dyes might be selectively bound to certain intracellular organelles. Possibility of binding to mitochondria was ruled out by co-staining **2** with commercial MitoTracker® Green FM on COS-7 cells (ESI,† Fig. S8). The intracellular location of **2** was eventually confirmed by co-staining with LysoTracker® Green DND-26, which showed excellent co-localization (Fig. 2 and ESI,† Fig. S16). The calculated Mander's correlation coefficients for probes **2a–2d** were >0.9 in all cell lines, indicating the exceptional lysosome specificity (ESI,† Fig. S9). Consistent results were also observed in the co-localization with

Table 1 Optical properties of probes **2a**–**2d**

Solvent	Property	Probe **2a**	**2b**	**2c**	**2d**
DCM	λ_{abs}	530 nm	531 nm	532 nm	542 nm
	λ_{em}	633 nm	632 nm	634 nm	641 nm
	(QY)	(0.15)	(0.16)	(0.12)	(0.17)
DMSO	λ_{abs}	479 nm	483 nm	481 nm	492 nm
	λ_{em}	638 nm	636 nm	638 nm	645 nm
	(QY)	(0.22)	(0.27)	(0.31)	(0.48)
EtOH	λ_{abs}	491 nm	495 nm	494 nm	507 nm
	λ_{em}	627 nm	628 nm	628 nm	637 nm
	(QY)	(0.13)	(0.15)	(0.19)	(0.21)
Water	λ_{abs}	468 nm	470 nm	471 nm	481 nm
	λ_{em}	632 nm	631 nm	630 nm	640 nm
	(QY)	(0.054)	(0.051)	(0.063)	(0.061)

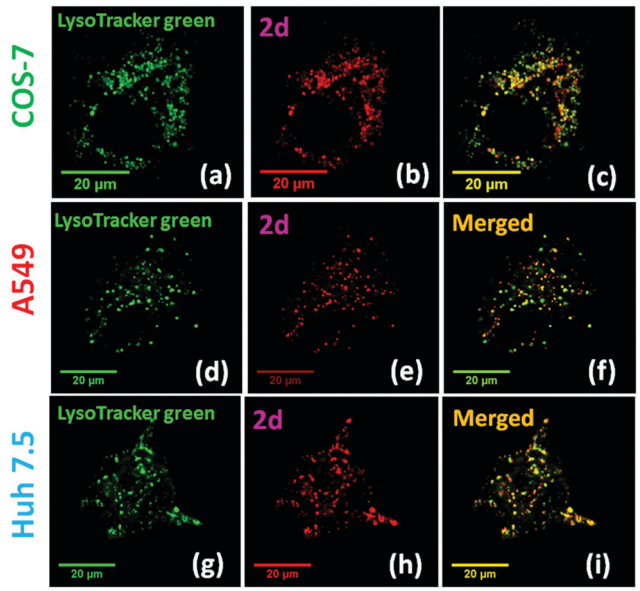

Fig. 2 Fluorescence confocal microscopy images of COS-7, A549 and Huh 7.5 cells incubated for 30 minutes with probe **2d** (500 nM) with LysoTracker® Green DND-26 (70 nM). Images (a), (d), and (g) shows fluorescence microscope images of LysoTracker® Green DND-26 (70 nM) images (b), (e), and (h) represent images of probe **2d**. Images (c), (f), and (i) represent overlapped figures for **2d** with LysoTracker® Green. Probe **2d** was excited with a 561 nm laser and Lysotracker® Green was excited with a 488 nm laser line. All images were obtained at 63× oil magnification. Mander's overlap coefficient calculated for **2d** was found to be 0.93, 0.94 and 0.90, respectively, in COS-7, A549 and Huh 7.5 cells (number of replicates = 3, n = 40 cells).

LysoTracker® Green DND-26 in HEK 293 cells (ESI,† Fig. S10) and in cancer cell lines (A549 and Huh 7.5), showing the probe's ability to visualize lysosome in live cells. The observed lysosome selectivity from **2** was in sharp contrast to the nucleus selectivity reported from **1**,[32] showing a large impact of the associated cyanine segment on the organelle selectivity.

The LC_{50} values for probe **2** were calculated to be in the 25–30 μM range by using CellTiter-Glow® luminescencent cell viability assay in COS-7 cells (ESI,† Fig. S22). The result further confirmed that these probes are suitable for biological cell studies since the working concentration of the probes are far below their calculated LC_{50} value. Bright fluorescent confocal microscopy images could be obtained when probe **2** concentration was as low as 100 nM (ESI,† Fig. S15).

Long term imaging: Lack of cellular pH perturbation, in addition to its low toxicity, raises possibility of using **2** for long term lysosome imaging. Thus, A549 cells were treated with **2d** (500 nM) over a period of 6 hours, which gave stable fluorescent confocal microscopy images (Fig. 3a and ESI,† Fig. S18). In sharp contrast, cells stained with commercial LysoTracker® Red DND-99 showed significant morphological changes and notable cell shrinkage after 1.5 hours (Fig. 4a and ESI,† Fig. S19). The fluorescence signals of **2d** and LysoTracker® Red was further analyzed by plotting their average fluorescence intensity *vs.* staining time (Fig. 3b). No apparent intensity change were observed from **2b** in A549 cells over a period of 6 hours.

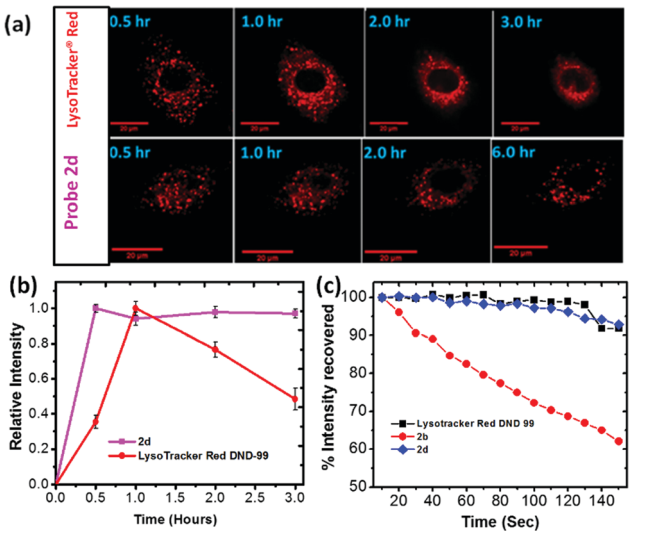

Fig. 3 (a) Time based photo-stability experiment for A549 cells incubated with **2d** (500 nM) and LysoTracker® Red DND-99 (100 nM) for 30 minutes. Images were obtained at 30 minutes intervals under consistent parameters of the microscope. Probe **2d** and LysoTracker® Red were excited with 561 nm laser. (b) Relative average fluorescence intensity obtained from A549 cells stained with probe **2d** (500 nM) and LysoTracker Red (70 nM) for a period of 3 hours. Probe **2d** and LysoTracker® Red were excited with a 561 nm laser. (c) The plot of recovered fluorescence intensity *versus* irradiation time calculated for LysoTracker® Red (100 nM), **2b** (100 nM) and **2d** (100 nM). All probes were stained in A549 cells, and excited with a 561 nm laser.

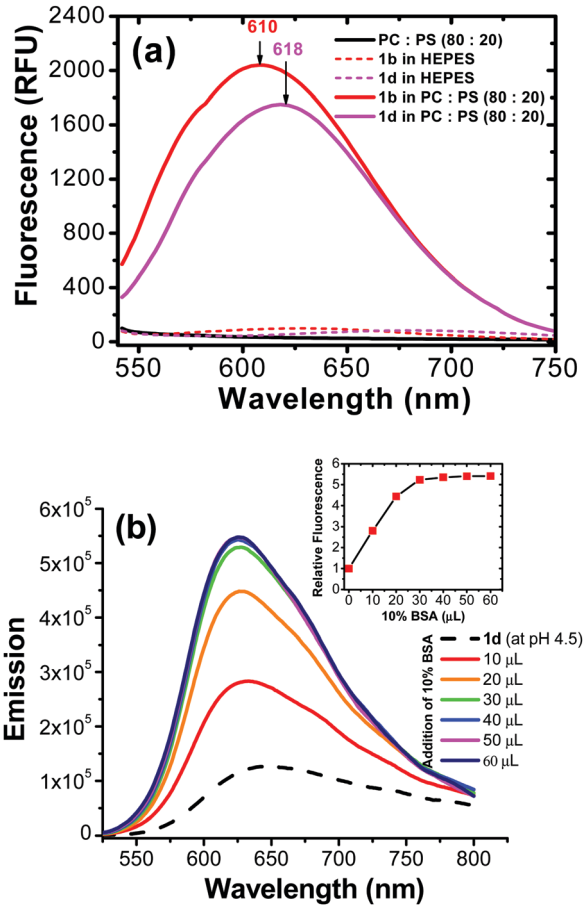

Fig. 4 (a) Fluorescence emission obtained for **2b** and **2d** (1×10^{-5} M) upon introduction in to 1 mM lipid vesicles (PC : PE 80 : 20) in HEPES buffer (pH = 7.4). Probes were excited at 530 nm. (b) Represents the fluorescence emission enhancement observed in **2d** (1×10^{-5} M) upon addition of 10% bovine serum albumin (BSA) in to an aqueous solution (pH 4.5) of probe **2d** (1×10^{-6} M). Probe **2d** was excited at 500 nm for emission collection.

However, LysoTracker® exhibited a significant decrease in relative intensity with time, which could be attributed to the fluorescence quenching due to pH elevation within lysosomes (*i.e.* alkalinizing effect). In another experiment, COS-7 cells were incubated with probe **2d** for 30 min and 24 h, and clear fluorescence signal was still observable from **2d** even after 24 h in comparison with initial confocal microscopy images (ESI,† Fig. S21). The ability of **2** in giving stable fluorescence signals in intracellular environment (*e.g.* on lysosomes, Fig. 3b) thus opened the possibility for long term imaging, due to elimination of pH sensitivity.

Photostability: Photostability was evaluated by studying the samples of A549 cells that were stained with **2b**, **2d** or LysoTracker® Red for 30 minutes separately. The resulting samples were continuously irradiated with a 561 nm laser on the microscope (ESI,† Fig. S23 and S24). The fluorescence intensity, averaged by measurement on samples ($n > 30$), was plotted as a function of irradiation time (Fig. 3c). Probe **2d** exhibited excellent stability in comparison with the commercial LysoTracker® Red, without showing significant photobleaching during the experiment period (Fig. 3c). The result also suggested that the substituent on the benzothiazolium segment had a large impact on the photostability of **2**. A possible reason for poor photostability of **2b** is attributed to possible photodegradation of the excited probe in the presence of molecular oxygen where singlet oxygen ($^1O_2$) or superoxide anion (O_2^-) upon interactions of the excited probe **2** with molecular oxygen (see ESI,† Fig. S28).[33,34] Therefore, relative electron density on cyanine N atom can affect their photostability (**2d** exhibited a greater photostability as a result of having electron rich benzyl substituent).[34]

Possible probe interaction: Since the probe structure does not include a basic amino group, the intriguing question is how the probe **2** was accumulated in cellular lysosomes. Since both pyrene and benzothiazolium segments are quite inert to protonation, the acidic environment in the organelle might not promote accumulation of **2** in the lysosome lumen. The hydrophobic nature of pyrene segment thus led us to assume that probe **2** might enter hydrophobic regions (*i.e.*, lysosomal membrane or lysosomal proteins) rather than the aqueous lysosomal lumen. One possibility is that **2** could be associated with the lysosomal membrane (hydrophobic region). In order to evaluate the hypothesis, we carried out a study involving *in vitro* generated lipid vesicles that can mimic an artificial phospholipid bilayer structure similar to cellular membranes. In the control experiment, probe **2** did not show any appreciable fluorescent signal in aqueous HEPES buffer (pH = 7.4). Interestingly, the pyrene-based molecules (**2b** and **2d**) exhibited a large fluorescent turn on in the presence of liposome vesicles (Fig. 4a). This observation

indicated that the possibility to associate with hydrophobic membrane components of the lysosome, generating fluorescence turn on signal. The assumption is consistent with the literature report where pyrene-based probes are able to stain biological membranes due to their hydrophobic nature.[30]

Fluorescence of **2** in different pH aqueous solutions revealed that emission was only slightly affected (about ±10%) in a wide pH range (pH = 3.2–11.4) (ESI,† Fig. S6). Since the fluorescence of **2** did not change significantly from neutral (pH ≈ 7.2) to acidic (pH ≈ 4.5 within lysosome lumen), in intracellular it is possible that the dye is binding to a hydrophobic region of lysosomes. In another experiment, an acidic aqueous solution of (pH = 4.5) probe **2d** was titrated with 10% bovine serum albumin (BSA). Interestingly, addition of BSA led to a significant fluorescent enhancement (≈600%) (Fig. 4b). It should be pointed out that BSA binding did not cause fluorescence enhancement in commercial LysoTracker® probes, since the PET effect from an amine group would be stronger in BSA than in acidic aqueous.[35] Therefore, interaction mechanism of the probe **2** in cellular lysosomes should be significantly different from that of acidotropic commercial LysoTracker® probes.

In conclusion, new fluorescent probes series have been successfully developed by coupling pyrene and benzothiazolium segments. In addition to bright red emission with large Stokes' shift ($\Delta\lambda > 130$ nm), the pyrene-based probes **2** exhibited the following attractive properties that are distinctive from the existing lysosome probes: (1) low cytotoxicity ($LC_{50} > 25$ μM); (2) large fluorescence turn on in hydrophobic environments, such as hydrophobic lysosomal lipid membrane, to enable wash-free staining; and (3) stable emission throughout a wide pH range (1.0–12.0), as the probe structure is insensitive to acidity. Although their structures do not contain an amino group, the new probes (**2a–2d**) exhibit remarkable selectivity for visualizing lysosomes in both healthy and tumor cells. By eliminating the "alkalinizing effect", the new probes have significant advantages over the existing commercial LysoTracker® probes and can be used for long term tracking of lysosome activity. This study points to the possibility of developing lysosome probes by targeting the lysosome membranes, rather than the acidic lysosome lumens where the enzymatic activities occur. Since probes **2** do not exhibit "alkalinizing effect" and exert minimal perturbation on the digestive activities of enzymes, they could be valuable tools for monitoring lysosome activities in biological research.

Y. P. acknowledges support from the University of Akron *via* Coleman endowment, and partial support from NIH (Grant no. 1R15GM126438-01A1). K. J. W. was supported by a NIH CBBI fellowship (T32GM075762). The imaging studies were supported by the Indiana University School of Medicine-South Bend Imaging and Flow Cytometry core (to R. V. S.).

Conflicts of interest

There are no conflicts to declare.

References

1 N. B. Yapici, Y. Bi, P. Li, X. Chen, X. Yan, S. R. Mandalapu, M. Faucett, S. Jockusch, J. Ju and K. M. Gibson, *Sci. Rep.*, 2015, **5**, 8576.
2 X. Chen, Y. Bi, T. Wang, P. Li, X. Yan, S. Hou, C. E. Bammert, J. Ju, K. M. Gibson, W. J. Pavan and L. Bi, *Sci. Rep.*, 2015, **5**, 9004.
3 C. de Duve and R. Wattiaux, *Annu. Rev. Physiol.*, 1966, **28**, 435–492.
4 T. Kirkegaard and M. Jäättelä, *Biochim. Biophys. Acta, Mol. Cell Res.*, 1793, **2009**, 746–754.
5 H. Maes and P. Agostinis, *Mitochondrion*, 2014, 58–68.
6 P. Honscheid, K. Datta and M. H. Muders, *Int. J. Radiat. Biol.*, 2014, **90**, 628–635.
7 P. Jiang and N. Mizushima, *Cell Res.*, 2014, **24**, 69.
8 X. He, J. Li, S. An and C. Jiang, *Ther. Delivery*, 2013, **4**, 1499–1510.
9 J. Reyjal, K. Cormier and S. Turcotte, *Advances in Experimental Medicine and Biology*, 2014, vol. 772, pp. 167–188.
10 F. M. Platt, *Nat. Rev. Drug Discovery*, 2004, **5**, 642–649.
11 R. Ashoor, R. Yafawi, B. Jessen and S. Lu, *PLoS One*, 2013, **11**, 82481.
12 M. Jaattela, *Oncogene*, 2004, **23**, 2746–2756.
13 P. Boya and G. Kroemer, *Oncogene*, 2008, **27**, 6434–6451.
14 T. Reinheckel, J. Deussing, W. Roth and C. Peters, *Biol. Chem.*, 2001, **382**, 735–741.
15 K. N. Balaji, N. Schaschke, W. Machleidt, M. Catalfamo and P. A. Henkart, *J. Exp. Med.*, 2002, **196**, 493–503.
16 U. Felbor, B. Kessler, W. Mothes, H. H. Goebel, H. L. Ploegh, R. T. Bronson and B. R. Olsen, *Proc. Natl. Acad. Sci. U. S. A.*, 2002, **99**, 7883–7888.
17 M. E. Guicciardi, M. Leist and G. J. Gores, *Oncogene*, 2004, **23**, 2881–2890.
18 R. P. Haugland, *The handbook: a guide to fluorescent probes and labeling technologies, molecular probes*, 2005.
19 G. Y. Wiederschain, *Biochemistry*, 2011, **76**, 1276.
20 X. Zhang, C. Wang, Z. Han and Y. Xiao, *ACS Appl. Mater. Interfaces*, 2014, **6**, 21669–21676.
21 H. Zhu, J. Fan, Q. Xu, H. Li, J. Wang, P. Gao and X. Peng, *Chem. Commun.*, 2012, **48**, 11766–11768.
22 H. M. Kim, M. J. An, J. H. Hong, B. H. Jeong, O. Kwon, J. Y. Hyon, S. C. Hong, K. J. Lee and B. R. Cho, *Angew. Chem., Int. Ed.*, 2008, **47**, 2231–2234.
23 B. Wang, S. Yu, X. Chai, T. Li, Q. Wu and T. Wang, *Chem. – Eur. J.*, 2016, **22**, 5649–5656.
24 Y. Han, M. Li, F. Qiu, M. Zhang and Y.-H. Zhang, *Nat. Commun.*, 2017, **8**, 1307.
25 X. Zhang, C. Wang, Z. Han and Y. Xiao, *ACS Appl. Mater. Interfaces*, 2014, **6**, 21669–21676.
26 D. Dahal, L. McDonald, X. Bi, C. Abeywickrama, F. Gombedza, M. Konopka, S. Paruchuri and Y. Pang, *Chem. Commun.*, 2017, **53**, 3697–3700.
27 Y. Niko, Y. Cho, S. Kawauchi and G. Konishi, *RSC Adv.*, 2014, **4**, 36480.
28 Y. Niko, S. Kawauchi and G. I. Konishi, *Chem. – Eur. J.*, 2013, **19**, 9760–9765.
29 Y. Niko, S. Kawauchi, S. Otsu, K. Tokumaru and G. I. Konishi, *J. Org. Chem.*, 2013, **78**, 3196–3207.
30 Y. Niko, P. Didier, Y. Mely, G. I. Konishi and A. S. Klymchenko, *Sci. Rep.*, 2016, **6**, 18870.
31 Y. Niko, H. Moritomo, H. Sugihara, Y. Suzuki, J. Kawamata and G. Konishi, *J. Mater. Chem. B*, 2015, **3**, 184–190.
32 C. S. Abeywickrama, K. J. Wijesinghe, R. V. Stahelin and Y. Pang, *Chem. Commun.*, 2017, **53**, 5886–5889.
33 C. Chen, B. Zhou, D. Lu and G. Xu, *J. Photochem. Photobiol., A*, 1995, **89**, 25–29.
34 X. Chen, X. Peng, A. Cui, B. Wang, L. Wang and R. Zhang, *J. Photochem. Photobiol., A*, 2006, **181**, 79–85.
35 K. A. Bertman, C. S. Abeywickrama, H. J. Baumann, N. Alexander, L. McDonald, L. P. Shriver, M. Konopka and Y. Pang, *J. Mater. Chem. B*, 2018, **6**, 5050–5058.

